

# Interchain Interactions Mediated by Br Adsorbates in Arrays of Metal–Organic Hybrid Chains on Ag(111)

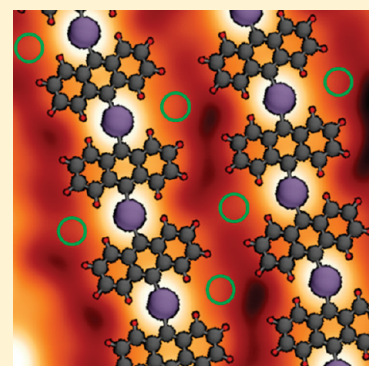
Jihun Park,<sup>†</sup> Kye Yeop Kim,<sup>‡</sup> Kyung-Hoon Chung,<sup>†</sup> Jong Keon Yoon,<sup>†</sup> Howon Kim,<sup>†</sup> Seungwu Han,<sup>‡</sup> and Se-Jong Kahng<sup>\*,†</sup>

<sup>†</sup>Department of Physics, Korea University, 1-5 Anam-dong, Seongbuk-gu, 136-713, Seoul, Korea

<sup>‡</sup>Department of Materials Science and Engineering, Seoul National University, Seoul 151-744, Korea

**S** Supporting Information

**ABSTRACT:** Interchain interactions in arrays of metal–organic hybrid chains were studied using scanning tunneling microscopy and ab initio calculations. The array of hybrid chains having a Ag–anthryl biradical were self-assembled by catalytic scission of Br–C bonds in 9,10-dibromoanthracene on Ag(111). An atomic model for the observed chain structures was proposed. Ag atoms in chains were alternately located at hollow sites, making slightly zigzagging structures. Between the hybrid chains, Br atoms located at hollow sites to form Br···H intermolecular bonds. Anthryl biradicals had two different apparent heights; this was explained by considering Br···H intermolecular bonds and intrachain steric repulsion. When a hybrid chain was laterally moved by manipulation techniques, Br adsorbates moved together with the chain, implying that they are stabilized by Br···H intermolecular bonds.



## 1. INTRODUCTION

Metal–organic hybrid structures have attracted much attention due to possible applications including gas storage, heterogeneous catalysis, and molecular separation.<sup>1,2</sup> Hybrid structures are primarily synthesized in solution phase but can be grown under vacuum conditions.<sup>3</sup> On metal surfaces, it has been reported that one-dimensional (1-D) metal–organic hybrid chains were grown via catalytic self-assembly processes.<sup>4–9</sup> When diiodinated (brominated) molecules were deposited on a Cu(111) surface, iodine (bromine) atoms were released from the molecules, thereby producing reactive biradicals. Cu adatoms available on the surface bridged two biradicals with C–I (C–Br) coordination bonds, forming 1-D Cu biradical hybrid chains. These hybrid chains were observed in different shapes (straights, zigzags, and circles) depending on the relative locations of two iodines (bromines) in a molecule.<sup>4–9</sup> It was considered that hybrid chains were intermediate steps in which to grow clean polymer chains or graphene nanoribbons in a vacuum.<sup>6,8,9</sup> In these previous reports, the observed hybrid chains often formed well-ordered arrays of two-dimensional (2-D) islands.<sup>4–6</sup> They made parallel 1-D structures with equal spacing of about 1 nm. Similar ordered 1-D structures were previously studied in atomic chains and molecular chains.<sup>10–12</sup> Such parallel chains imply that there are mechanisms that mediate attractive or repulsive interactions between hybrid chains. These mechanisms could be examined by considering atomic structures and charge distributions of hybrid chains in relation to substrate lattices. However, such a study has not been reported for hybrid 1-D structures in the literature.

We studied the atomic structures of hybrid chains and their intra- and inter-molecular interactions using a scanning tunneling microscope (STM). Hybrid chains were spontaneously grown by depositing 9,10-dibromoanthracene (DBA) on Ag(111). A slightly zigzagging atomic model for the observed structures was proposed. Br adsorbates between hybrid chains form Br···H intermolecular bonds, thereby mediating interchain interactions. Two different apparent heights were observed in anthryl biradicals (AB) in the hybrid chains. This was explained by considering Br···H intermolecular bonds and steric repulsion between neighboring ABs.

## 2. EXPERIMENTAL SECTION

Our experiments were carried out with a home-built low-temperature STM operated at a temperature of 80 K in an ultrahigh vacuum. The base pressure was less than  $1 \times 10^{-10}$  Torr. The single-crystal Ag(111) surface was prepared by several cycles of Ne<sup>+</sup> ion sputtering and annealing at 800 K. The surface cleanliness was checked by STM observation of an atomically flat Ag(111) surface. Commercially available 9,10-dibromoanthracene (Tokyo Chemical Industry, Japan) was outgassed in a vacuum for several hours and then deposited on the Ag(111) at room temperature for 2 min by thermal evaporation using an alumina-coated evaporator. The flux was controlled to 0.01 monolayer per

**Received:** April 4, 2011

**Revised:** July 4, 2011

**Published:** July 05, 2011

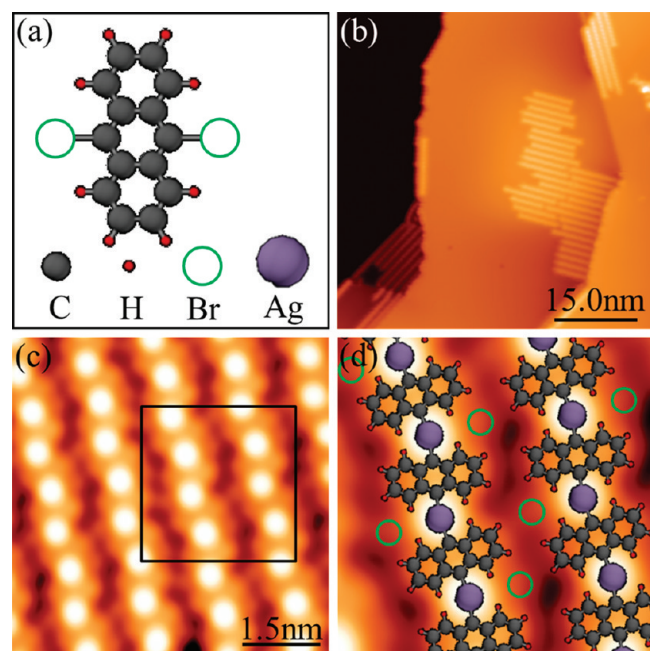


**Figure 1.** (a) Chemical structures of a 9,10-dibromoanthracene (DBA) molecule. (b) Typical STM image measured at 80 K after DBA molecules were deposited at room temperature on Ag(111) ( $V_S = 1.0$  V,  $I_T = 0.1$  nA,  $57.5 \times 57.5$  nm<sup>2</sup>). (c) STM image zoomed in on an island. 2-D island made of 1-D hybrid chains of a Ag–anthryl biradical (AB) ( $V_S = 1.0$  V,  $I_T = 0.1$  nA,  $6.1 \times 6.1$  nm<sup>2</sup>). (d) Ag–AB 1-D hybrid chain model overlapped with an enlarged STM image denoted by the square in (c).

minute. STM images were obtained using constant-current mode with a Pt/Rh tip while the sample temperature was kept at 80 K.

### 3. THEORETICAL CALCULATIONS

We performed ab initio calculations at the level of density functional theory (DFT) with the VASP code.<sup>13</sup> The generalized gradient approximation with the Perdew–Burke–Ernzerhof (PBE) functional<sup>14</sup> was used, and the energy cutoff for the plane wave basis was set to 500 eV. Other details in the computational setup follow our recent publication.<sup>15</sup> To describe nonbonding interactions between the molecules, especially of van der Waals type, an empirical correction scheme proposed by Grimme. et al. was adopted.<sup>16</sup> A simulation cell containing one Ag–anthryl biradical chain, two Br adsorbates, and two Ag atoms under the Br adsorbates was adopted to describe the periodic structure. The underlying Ag atoms were introduced to imitate the Ag substrate. The height of the simulation box perpendicular to the molecule plane was fixed to 10 Å, while the lateral cell parameters were optimized such that the residual stress was reduced under 1 kbar.

### 4. RESULTS AND DISCUSSION

The chemical structure of a DBA molecule is shown in Figure 1a. When DBA molecules were deposited at room temperature on Ag(111), 2-D islands made of 1-D chains were observed, as shown in Figure 1b and c. A chain was made of bright dots interspaced by dark bars. Similar to other brominated (iodinated) molecules, Br atoms in the DBA were detached and subsequently replaced by Ag atoms to form 1-D chains.<sup>4–9</sup> Ag atoms were supplied from mobile adatoms available on Ag(111)

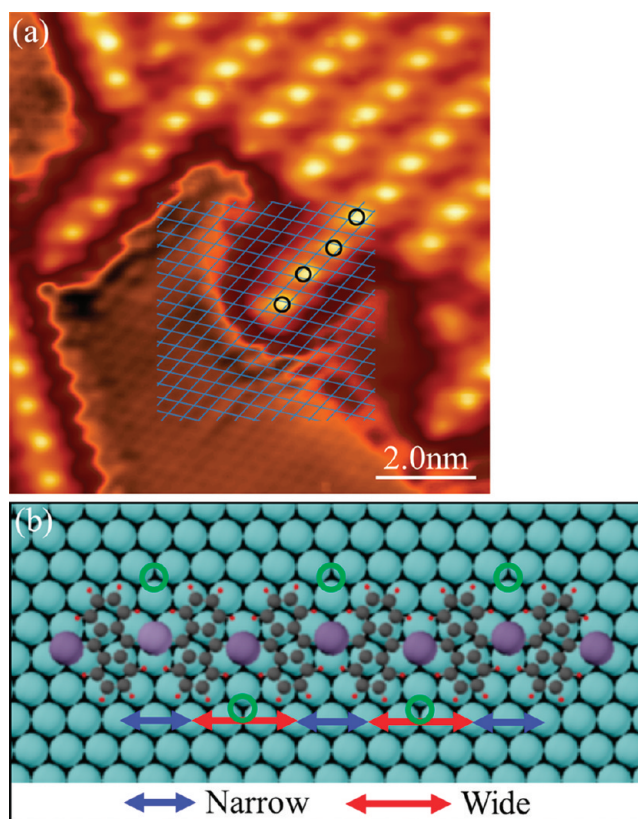


**Figure 2.** (a) STM image that resolves Ag atoms in the substrate and hybrid chains simultaneously. The grid is the lattice of the Ag(111) substrate, and the circles are fcc and hcp hollow sites ( $V_S = -0.1$  V,  $I_T = 0.5$  nA,  $9.6 \times 9.6$  nm<sup>2</sup>). (b) An atomic model for a hybrid chain. The red (blue) arrows are wide (narrow) gaps of ABs. Gray, red, green, and violet represent carbon, hydrogen, bromine, and silver, respectively.

at room temperature or from surface atoms pulled during the reaction processes.<sup>17</sup> We assigned dots as Ag atoms and bars as anthryl biradicals (ABs). A Ag–AB unit repeated to form hybrid chains, as shown in Figure 1d. Isolated metal adatoms are usually imaged with an apparent height less than that of aromatic molecules. However, the situation can be changed when a metal adatom forms a contact to an aromatic molecule.<sup>18</sup> Apparent heights will be determined by modified electronic structures of combined systems. In other hybrid structures, bright dots were assigned as metal adatoms, and less bright parts (bars) were assigned as aromatic molecules.<sup>4,6,7,17</sup> These hybrid chains were observed along three equivalent crystallographic directions,  $[1\bar{1}0]$ ,  $[10\bar{1}]$ , and  $[01\bar{1}]$ .

Figure 2a shows a STM image that simultaneously resolved the substrate lattice and hybrid chains. On the basis of this image, we propose a detailed atomic model for a hybrid chain on Ag(111), as shown in Figure 2b. The model consists of three components, Ag, AB, and Br. Ag atoms alternately adsorb at face-centered cubic (fcc) and hexagonal close-packed (hcp) hollow sites. They are slightly zigzagged with an angle of  $166.8^\circ$ , and the nearest-neighbor distance of Ag atoms in one chain is 0.73 nm, consistent with experimental observations ( $0.74 \pm 0.05$  nm and  $166 \pm 3^\circ$ ). An AB is bridged between two Ag atoms. The long axes of ABs are alternately tilted by  $6.6^\circ$  from the direction perpendicular to a chain axis. Two neighboring ABs in a chain make a wide and a narrow gap, as shown in Figure 2b. In a wide

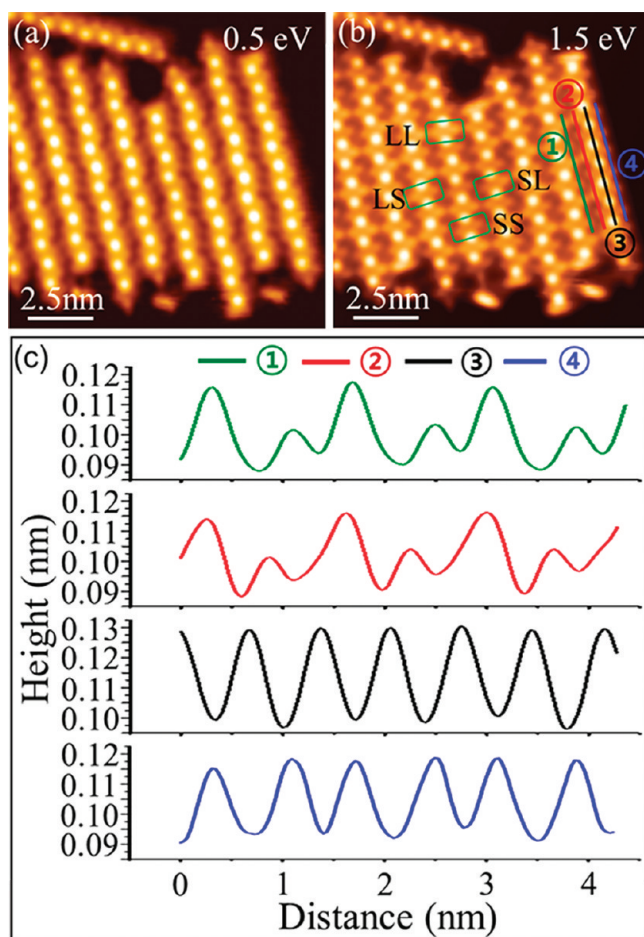


**Figure 3.** STM images obtained at (a) 0.5 and (b) 1.5 eV ( $I_T = 0.4$  nA,  $12.1 \times 12.1$  nm<sup>2</sup>). (c) Profiles along the hybrid chains denoted in (b). The black line is the profile along the Ag atoms, and the other three profiles are taken along half-ABs in an island (green and red lines) and at the end of an island (blue line). We used a modified color scale in (a) and (b) to clearly represent the height differences in anthryl biradicals. In the Supporting Information, the same images are provided with a typical color scale.

gap, a Br atom is located at a hollow site; however, no Br atoms locate in a narrow gap. In our model, three hexagon rings carrying  $\pi$ -electrons in ABs sit at bridge sites. This is consistent with previous reports.<sup>19,20</sup> We have considered the case that DBA radicals coordinate to Ag surface atoms that are slightly pulled out from the surface. In such structures, the locations of Ag atoms in a surface atomic lattice should be top sites. However, our STM data better match the model with Ag atoms in hollow sites.

STM images of hybrid chains have energy dependence. Two STM images obtained at the same location with different voltages are shown in Figure 3a and b. Ag atoms looked bright in both STM images. Br atoms were visible at 0.5 eV but invisible at 1.5 eV. ABs were better resolved at 1.5 eV than at 0.5 eV. When we closely looked at the STM images obtained at 1.5 eV, as shown in Figure 3b, we unexpectedly found that there were two different apparent heights in the ABs. Figure 3c shows the profiles along four lines denoted in a STM image of (b). A profile across Ag atoms has a single apparent height of 0.13 nm. Two profiles across the ABs in the islands have alternating apparent heights of either 0.12 or 0.10 nm. The last profile across the ABs at the edge of islands shows a single apparent height of 0.12 nm.

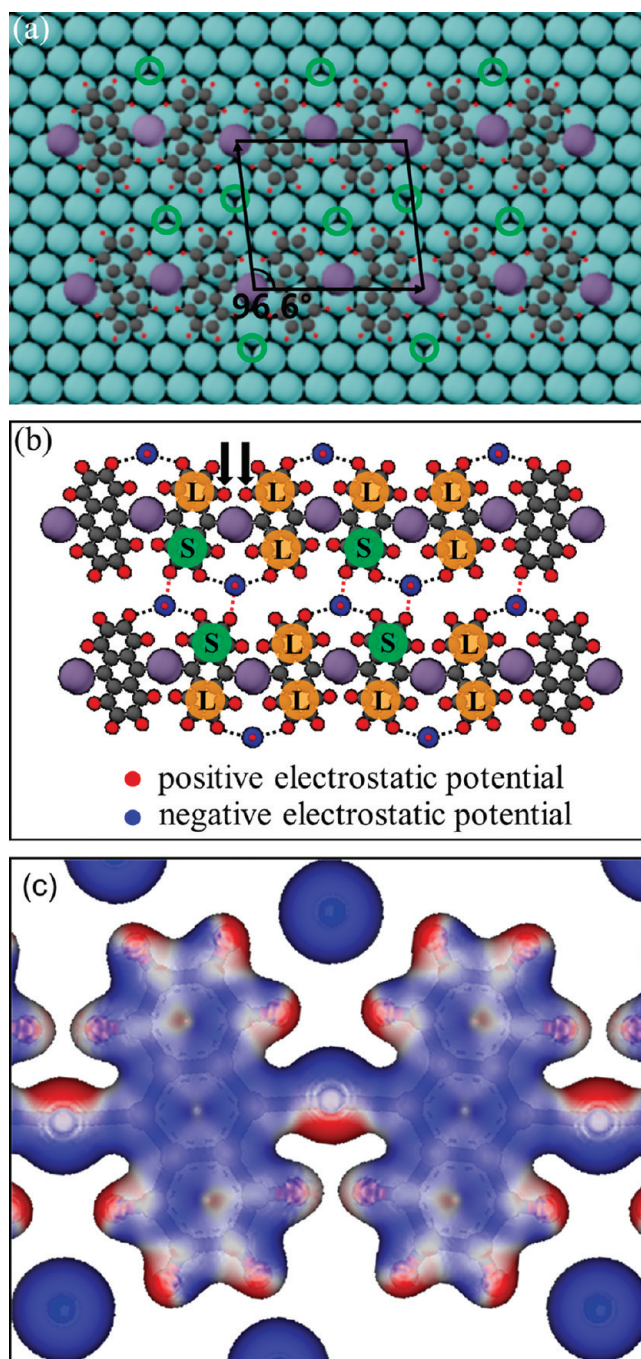


**Figure 4.** (a) Atomic model for two Ag–AB hybrid chains. The parallelogram with two unit vectors is the unit cell. (b) Atomic model with schematic electrostatic potentials in H atoms and Br adsorbates (red represents positive electrostatic potentials, and blue represents negative electrostatic potentials). The Br $\cdots$ H distances of the red (black) dashed lines are 0.28 nm (0.30 nm). The distance between two H atoms denoted by arrows is 0.18 nm. (c) Calculated molecular electrostatic potential distributions of a Ag–anthryl biradical hybrid chain and Br adsorbates at the isodensity surface, shown in red (positive) and blue (negative).

This single apparent height of the ABs took place only at the edge of the islands. At the inner part of 2-D islands, the apparent heights of ABs always alternated. We also found that a single AB had four different configurations, SL, LS, SS, and LL, as denoted

in Figure 3b. Namely, an AB denoted by SL (LS) has a small (large) apparent height at the left half and a large (small) apparent height at the right half. SS (LL) means that both ABs are small (large). These two different apparent heights with four configurations cannot be explained using the single chain model shown in Figure 2b.

To explain the two observed apparent heights, we considered a two-chain model, as shown in Figure 4a, and intermolecular interactions caused by electrostatic potential distributions, shown in Figure 4b. It has been reported that halogen adsorbates on metal surfaces took mostly negative electrostatic potentials due to their large electronegativity compared to metal atoms.<sup>21,22</sup> (Although they also have a small region of positive potentials at the top of adsorbates, this does not affect lateral intermolecular interactions.) Meanwhile, H atoms in the ABs have positive electrostatic potentials due to their small electronegativity compared to that of C atoms. Therefore, it is clear that a H atom and a neighboring Br adsorbate have an attractive interaction. From the model shown in Figure 4a, we estimated that the distances between a H and a Br was 0.28 nm (the red dotted line in Figure 4b) or 0.30 nm (the black dotted line in Figure 4b). These distances were close enough to form a Br···H intermolecular bond when compared to the sum of the van der Waals radii of the two atoms, 0.31 nm. With this intermolecular bond, half-ABs can be divided into two types. (Because an AB has two independent apparent heights, we considered a half-AB.) Some half-ABs have two Br···H bonds, whereas other half-ABs have only one Br···H bond. In addition to these Br···H bonds, we also considered intrachain repulsion between two H atoms to explain the two different observed apparent heights of half-ABs. In a narrow gap of two ABs, two H atoms (denoted by arrows in Figure 4b) are so close that they may exhibit steric repulsion. In the model shown Figure 4a, the distance between two H atoms is 0.18 nm, which is smaller than the sum of the van der Waals radii of two H atoms, 0.24 nm. With this intrachain repulsion and Br···H bond, we can explain why some half-ABs have large apparent heights while others have small apparent heights. Because two H atoms are under steric repulsion, one of the half-ABs is likely to be lifted from the surface. Then, we must consider which one will be lifted. Half-ABs with one (two) Br···H bond(s) are mechanically ill (well)-defined. Ill-defined half-ABs are lifted to have a large apparent height, and well-defined half-ABs have a small apparent height. With this mechanism, we could have three configurations, LS, LL, and SL, as shown in Figure 4b. However, we could not have an SS configuration. In fact, the SS configuration can easily be made by considering a three- or four-chain model (see Supporting Information). The apparent height of half-ABs at the outer part of the chain at the edge of the islands will stay large. They have one Br···H bond and may be under vibration with antipair correlation, thus explaining the observed single apparent height at the end-ABs shown in Figure 2c. Until now, we considered that the apparent height difference could be caused by geometry. We could not avoid the possibility that the apparent height difference could be related to the electronic structures of half-ABs.

To confirm the structure and potential distribution of the system, we performed *ab initio* calculations based on density functional theory. In calculation, all of the atoms in a chain and the Br atoms were confined to a plane. A Br atom formed a covalent bond to a Ag atom in the direction perpendicular to the plane to simulate the effect of the substrate. Figure 4c shows the electrostatic potential map on the isosurfaces to be 0.003 e/Bohr<sup>3</sup>, superimposed on the atomic structure relaxed by the calculation. The zigzag structure of Ag–Ag with a distance of 0.73 nm and an

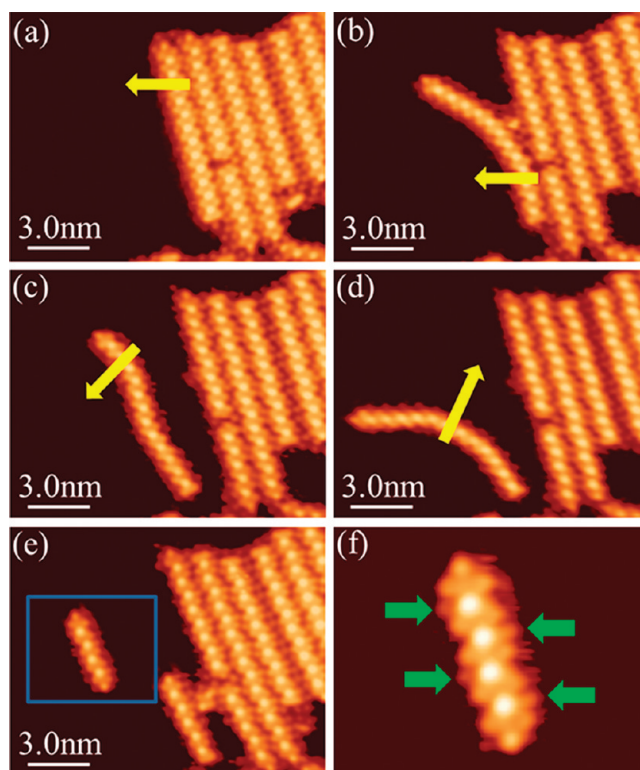


**Figure 5.** STM images obtained between consequent manipulation experiments (manipulation conditions:  $V_S = 10$  mV,  $I_T = 20$  nA). (a) Initially, self-assembled Ag–AB hybrid chains formed a 2-D island. The yellow arrow represents the tip movement of each manipulation step. (b,c) Ag–AB hybrid chain detached from a 2-D island. (d) The detached chain was bent and (e) cut off [(a–e)  $V_S = 0.5$  V,  $I_T = 1$  nA,  $15.3 \times 12.1$  nm<sup>2</sup>]. (f) Close-up STM image denoted by the square in (e) ( $V_S = 0.5$  V,  $I_T = 1$  nA,  $6.1 \times 4.6$  nm<sup>2</sup>). A hybrid chain detached from an island has Br adsorbates denoted by green arrows in (f).

angle of 172.0° was reproduced in reasonable agreement with experimental observations (0.73 nm and 166.8°, respectively). The angle is larger than that of Figure 2a because of the steric effect between two H atoms confined to a plane in the calculation. Two close H atoms in a narrow gap indeed show almost neutral electrostatic potential, implying steric repulsion. The calculated potential map shows the other essential features discussed in Figure 4b. Br atoms are attracted by H atoms, with the Br···H distance of 0.27 or 0.29 nm, slightly shorter than that of the model in Figure 2a. The net energy gain caused by the Br···H intermolecular interactions was estimated by the relation

$$E_{\text{gain}} = E_{\text{chain:BrAg}} - E_{\text{chain}} - 2XE_{\text{BrAg}} \quad (1)$$

Here,  $E_{\text{chain:BrAg}}$  represents the total energy of the structure including a hybrid chain and two Br–Ag.  $E_{\text{chain}}$  represents the total energy of a hybrid chain, and  $E_{\text{BrAg}}$  does that of a Br–Ag structure. The net gain in our calculation was about 800 meV per unit cell. Because the unit cell has six Br···H bonds, the strength of a Br···H bond is about 130 meV. This is stronger than the Br···H bond in the C–Br···H–C configuration, 70 meV with a distance of 0.27 nm in previous reports.<sup>15</sup> Because Ag has an electronegativity (1.93) smaller than that of C (2.55), Br adsorbates on Ag(111) may have stronger Br···H bonds than those in the C–Br···H–C configuration.

To know the stability of hybrid chains and Br···H intermolecular bonds, STM manipulations were performed to laterally

move a hybrid chain. As shown in Figure 5, a hybrid chain was detached from a 2-D island and moved farther using the STM tip. Because the hybrid chain was quite long, it was necessary to manipulate the upper and lower parts of the hybrid chain separately to obtain a translational displacement. The hybrid chain was slightly bent during these processes but retained its overall adsorption structures, implying that it is a flexible but robust structure. We were also able to break a hybrid chain into two parts. To break the hybrid chain, the STM tip was brought closer by about 0.02 nm to the hybrid chain than the case of lateral manipulation. Br adsorbates were still observed in the wide gaps of ABs after the manipulations, as shown in Figure 5f, which was a little surprising because they were not covalently bonded to the hybrid chains. Possibilities are that Br adsorbates either moved together with the hybrid chains or underwent detachment-rejoining processes. In the second case, Br adsorbates were left behind when a hybrid chain was moved by the STM tip and then moved around to find a new stable position. Br adsorbates could not find stable positions other than the original wide gap locations.

## 5. CONCLUSION

In summary, an array of Ag–AB hybrid chains were self-assembled on Ag(111). An atomic model consisting of Ag, AB, and Br was proposed. Between hybrid chains, Br atoms located at hollow sites to form Br···H intermolecular bonds. The two observed apparent heights of half-ABs were explained by considering Br···H intermolecular bonds and steric repulsion. These were well-reproduced by first-principles studies. Br adsorbates that interact strongly with H atoms of ABs in two neighboring hybrid chains play a role in mediating the interchain interactions.

## ■ ASSOCIATED CONTENT

Supporting Information. Figure of configurations and typical color scale images of Figure 3a,b. This material is available free of charge via the Internet at <http://pubs.acs.org>.

## ■ AUTHOR INFORMATION

### Corresponding Author

\*Tel: (+82) 2-3290-3109. Fax: (+82) 2-922-3484. E-mail: [sjkahng@korea.ac.kr](mailto:sjkahng@korea.ac.kr).

## ■ ACKNOWLEDGMENT

The authors gratefully acknowledge financial support from the National Research Foundation of Korea and from the Ministry of Education Science and Technology of the Korean government (Grants 2005-2002369, 2007-0054038, 2010-0025301, 2010-0018781). K.Y.K. and S.H. were supported by the Basic Science Research Program though the National Research Foundation of Korea (NRF) funded by the Ministry of Education, Science and Technology of Korea (2010-0011085).

## ■ REFERENCES

- (1) MacGillivray, L. *Metal–Organic Frameworks: Design and Application*; John Wiley & Sons, Inc.: Hoboken, NJ, 2010.
- (2) Mann, S. *Nat. Mater.* **2009**, *8*, 781–792.
- (3) Barth, J. V. *Surf. Sci.* **2009**, *603*, 1533–1541.
- (4) McCarty, G. S.; Weiss, P. S. *J. Phys. Chem. B* **2002**, *106*, 8005–8008.

- (5) McCarty, G. S.; Weiss, P. S. *J. Am. Chem. Soc.* **2004**, *126*, 16772–16776.
- (6) Lipton-Duffin, J. A.; Ivasenko, O.; Perepichka, D. F.; Rosei, F. *Small* **2009**, *5*, 592–597.
- (7) Walch, H.; Gutzler, R.; Sirtl, T.; Eder, G.; Lackinger, M. *J. Phys. Chem. C* **2010**, *114*, 12604–12609.
- (8) Villagómez, C. J.; Sasaki, T.; Tour, J. M.; Grill, L. *J. Am. Chem. Soc.* **2010**, *132*, 16848–16854.
- (9) Cai, J.; Ruffieux, P.; Jaafar, R.; Bieri, M.; Braun, T.; Blankenburg, S.; Muoth, M.; Seitsonen, A. P.; Saleh, M.; Feng, X.; Müllen, K.; Fasel, R. *Nature* **2010**, *466*, 470–473.
- (10) Stekolnikov, A. A.; Bechstedt, F. *Phys. Rev. Lett.* **2008**, *100*, 196101.
- (11) Barth, J. V.; Weckesser, J.; Trimarchi, G.; Vladimirova, M.; Vita, A. D.; Cai, C.; Brune, H.; Günter, P.; Kern, K. *J. Am. Chem. Soc.* **2002**, *124*, 7991–8000.
- (12) Schmitz, C. H.; Ikononov, J.; Sokolowski, M. *J. Phys. Chem. C* **2009**, *113*, 11984–11987.
- (13) Kresse, G.; Hafner, J. *Phys. Rev. B* **1993**, *47*, 558.
- (14) Perdew, J. P.; Burke, K.; Ernzerhof, M. *Phys. Rev. Lett.* **1996**, *77*, 3865.
- (15) Yoon, J. K.; Son, W.-J.; Chung, K.-H.; Kim, H.; Han, S.; Kahng, S.-J. *J. Phys. Chem. C* **2011**, *115*, 2297–2301.
- (16) Grimme, S. *J. Comput. Chem.* **2004**, *25*, 1463–1473.
- (17) Bieri, M.; Nguyen, M.-T.; Gröning, O.; Cai, J.; Treier, M.; Ait-Mansour, K.; Ruffieux, P.; Pignedili, C. A.; Passerone, D.; Kastler, M.; Müllen, K.; Fasel, R. *J. Am. Chem. Soc.* **2010**, *132*, 16669–16676.
- (18) Nazin, G. V.; Qui, X. H.; Ho, H. *Science* **2003**, *302*, 77–81.
- (19) Wan, L.-J.; Itaya, K. *Langmuir* **1997**, *13*, 7173–7179.
- (20) Lukas, S.; Witte, G.; Wöll, Ch. *Phys. Rev. Lett.* **2002**, *88*, 028301.
- (21) Gava, P.; Kokalj, A.; Gironcoli, S.; Baroni, S. *Phys. Rev. B* **2008**, *78*, 165419.
- (22) Peljhan, S.; Kokalj, A. *J. Phys. Chem. C* **2009**, *113*, 14363–14376.